8th International Conference on Photonic Technologies LANE 2014

Surface structuring with ultra-short laser pulses: Basics, limitations and needs for high throughput

B. Neuenschwander[a],*, B. Jaeggi[a], M. Schmid[a], G. Hennig[b]

[a]Bern University of Applied Sciences, Institute for Applied Laser, Photoncis and Surface Technologies ALPS, Pestalozzistrasse 20, CH-3400 Burgdorf, Switzerland
[b]Daetwyler Graphics, Flugplatz, CH-3368 Bleienbach, Switzerland

- Invited Paper -

Abstract

The interest using ultra-short pulsed laser systems for industrial applications increased remarkably as reliable high power systems with average power exceeding several 10W became available, facilitating the development of high throughput processes. Exhausting the potential of these systems demands an optimized process and an adapted process strategy as well. For surface structuring it can be shown that in case of metals and many other materials, the ablation process itself shows a maximum efficiency at an optimum fluence. The corresponding removal rate directly scales with the average power and depends on the threshold fluence and the energy penetration depth into the material. These parameters are material depending but they change with the pulse duration and are also subject to incubation effects. Working at the optimum point with highest efficiency and keeping the high machining quality sets conditions for the process strategy which can only be fulfilled by either very high marking speeds, not available with common beam guiding systems, or high spot areas as they can e.g. achieved with multi-spots by a diffractive optical element or a spatial light modulator.

---

* Corresponding author. Tel.: +41-34-426-42-20; fax: +41-34-423-15-13 .
  E-mail address: beat.neuenschwander@bfh.ch

1. Introduction

Ultra-short pulsed laser systems show clear advantages concerning machining quality, heat affected zone or debris as it has been shown in many publications during the last years. The recent developments of laser systems go into different directions.

- Firstly towards kW average power as reported in [1,2] for fs-pulses (based on the innoslab technology) and shown in [3] for ps-pulses (based on a thin-disk amplifier).
- Secondly to more cost effective fiber based systems without chirped pulse amplification (CPA). These systems normally have pulse durations of a few 10 ps [4,5,6] but also 11 ps were already demonstrated [7] by using a gain-switched diode as seed source.
- Thirdly industry ready sub-ns Q-switched systems with pulse durations of several 100 ps are available on the market.
- Moreover also fiber lasers having pulse durations of only a few ns may be very attractive due its cost effectiveness and reliability.

On the other hand, also the process control is of very high importance and has to be adapted to the laser system as well as to the process itself. Today machines are using mechanical linear and rotation axes as well as galvo scanners or combinations of both. Acousto-optic deflectors, fast rotating cylinders or polygon wheels offer high marking speeds and diffractive optical elements (DOE) or spatial light modulators (SLM), in combination with linear axes or galvo scanners, can be used for parallel processing.

A potential user has therefore to choice from a wide range of laser systems with different parameters, beam guiding systems and process control technologies. But only appropriate combinations guarantee an economical process which can really take benefit from the advantages of short and ultra-short pulses for laser micro-machining. The following work is mainly focused on surface structuring of metals and will discuss some basics of the ablation process, will describe the influence of the pulse duration and will show how the process efficiency can be optimized. Based on the findings the needs to obtain high throughput will be formulated and actual technologies to meet the corresponding requirements will be presented.

2. Ablation process

2.1. Theoretical background

In contrast to longer pulses, where for metals the energy transport into the material is described by heat conduction, electron and lattice temperature have to be treated separately in the case of ultra-short pulses [8-12]. In a first approximation the absorbed energy per unit volume can be assumed to exponentially drop with the distance to the surface [10] and as a consequence the often reported logarithmic ablation law results:

$$z_{abl} = \delta \cdot \ln\left(\frac{\phi}{\phi_{th}}\right) \qquad (1)$$

With the ablation depth z_{abl}, the applied fluence ϕ, the threshold fluence ϕ_{th} and the energy penetration depth δ. It has further been shown that the time for the energy transfer from the free electrons to the lattice, the electron-phonon thermalization time, amounts a few ps [13,14] in the case of metals. A further reduction of the pulse duration will therefore not lead to additional benefits in terms of the threshold fluence [13], rather it can lead to a reduced precision and to increased unwanted plasma effects [14,15] at high fluences. In contrast to the threshold fluence, the energy transport into the material well depends on the pulse duration also for pulses shorter than the thermalization time. Depending on the applied fluence and the pulse duration the energy transport into the material is dominated either by the optical penetration depth or the electron heat penetration depth which depends on the pulse duration [9-12].

For a pulsed Gaussian beam with pulse energy E_p and spot radius w_0 the peak fluence in the center of the beam reads $\phi_0 = 2 \cdot E_P/(\pi \cdot w_0^2)$ and the local fluence is given by $\phi(r) = \phi_0 \cdot \exp(-2 \cdot r^2/w_0^2)$. Applying (1) leads to the local ablation depth $z(r)$ and to the ablated volume ΔV per pulse which reads [16,17]:

$$\Delta V = \frac{1}{4} \cdot \pi \cdot w_0^2 \cdot \delta \cdot \ln^2\left(\frac{\phi_0}{\phi_{th}}\right) \qquad (2)$$

Assuming that for multiple pulses the behavior of each pulse is not influenced by the leading pulse leads to an easy calculation of the volume removal rate $\dot{V}$ (ablated volume per time) as a function of the average power P_{av} and the repetition rate f [17]:

$$\dot{V} = \frac{1}{4} \cdot f \cdot \delta \cdot \pi \cdot w_0^2 \cdot \ln^2\left(\frac{2 \cdot P_{av}}{f \cdot \pi \cdot w_0^2 \cdot \phi_{th}}\right) \qquad (3)$$

Alternatively the removal rate per average power can be expressed in terms of the peak fluence ϕ_0 [18]:

$$\frac{\dot{V}}{P_{av}} = \frac{1}{2} \cdot \frac{\delta}{\phi_0} \cdot \ln^2\left(\frac{\phi_0}{\phi_{th}}\right) \qquad (4)$$

Fig. 1 shows this situation for stainless steel (1.4301), 10 ps pulses with 1064nm wavelength and a spot radius of $w_0 = 29$ μm. The graphs clearly illustrate that the ablation process shows an optimum point with highest efficiency and therefore maximum removal rate [17,19]. A short calculation leads to:

$$\left.\frac{\dot{V}}{P_{av}}\right|_{max} = \frac{2}{e^2} \cdot \frac{\delta}{\phi_{th}} \qquad (5)$$

This maximum removal rate is obtained at an optimum peak fluence $\phi_{0,opt}$ or repetition rate f_{opt}:

$$\phi_{0,opt} = e^2 \cdot \phi_{th} \qquad \frac{f_{opt}}{P_{av}} = \frac{2}{e^2} \cdot \frac{1}{\pi \cdot w_0^2 \cdot \phi_{th}} \qquad (6)$$
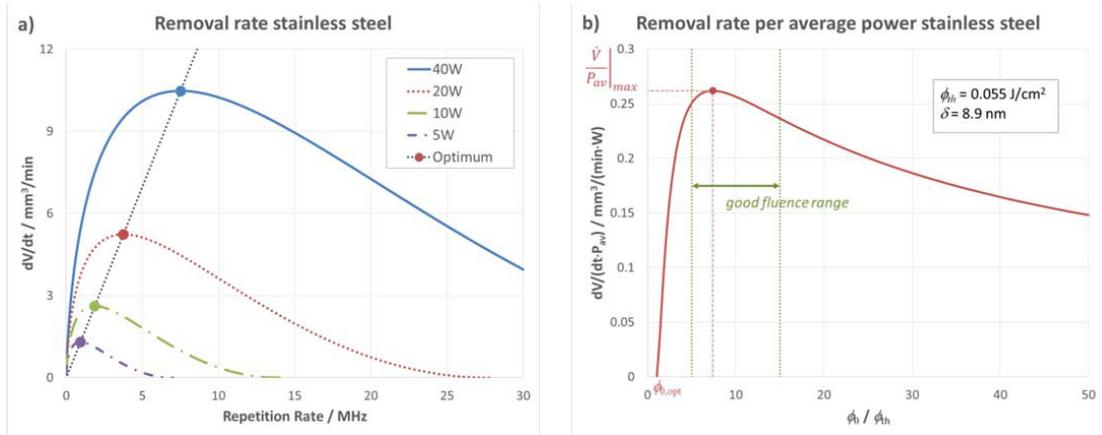

Fig. 1. (a) Removal rate for stainless steel for different average powers as a function of the repetition rate and a spot radius of $w_0 = 29$ μm; (b) Removal rate per average power for stainless steel as a function of the peak fluence ϕ_0.

Hence, following this simple model, the ablation process linearly scale with the average power if the fluence ϕ_0 (i.e. the pulse energy) is kept at its optimum value (6). Working at higher or lower peak fluences leads to a reduced efficiency (Fig. 1b) and a reduced quality for too high fluences [18]. Keeping ϕ_0/ϕ_{th} between 5 and 15 may represent a rough rule of tomb. For most metals this leads to quite low fluences and therefore high repetition rates or spot sizes are needed when working at high average power as shown in table 1 and as it will also be discussed later.

Table 1. Summary of optimum repetition rate depending on the spot radius and the average power.

Spot radius / μm	f_{5W} / MHz	f_{10W} / MHz	f_{20W} / MHz	f_{40W} / MHz
29	1.01	1.92	3.8	7.5
20	1.95	3.92	7.83	15.7
10	7.83	15.7	62.7	188

Care has to be taken if different situations, e.g. two materials or two pulse durations, are compared. E.g. the value of the threshold fluence often decreases with shorter wavelengths but if the energy penetration depth is also reduced this will not lead to a higher removal rate following (6). Another example is the use of pulse bursts, e.g. in [20] removal rates obtained in steel for average powers of 50W and repetition rates between 200kHz and 1MHz were compared for single pulses and bursts with 6, 8 and 10 pulses bursts at the same repetition rate (for the burst). It was found that the removal rate can be increased from 1.2mm³/min for single pulses at repetition rate of 200kHz up to 11.5mm³/min for 10 pulses per burst at 1MHz repetition rate. This gain in the removal rate can be well explained with the fact that the energy is distributed among a higher number of pulses, i.e. the same removal rate should also be obtained with single pulses at a repetition rate of 10 MHz. From the data published in [20] the energy of a single pulse in the burst was calculated and the least square fit with the model (4) to this data (see Fig. 2c) confirms this assumption. To back up the presented model different kind of experiments were performed. Fig. 2a) show a result from marking lines with different repetition rates but constant pulse-pulse distance [17,19,21,22] and fig. 2b) one from machining squares [18,23] with different fluences. All three graphs show the good agreement between the presented model and measured data.

The two most important material parameters describing the ablation process are therefore the threshold fluence ϕ_{th} and the energy penetration depth δ. Both can be deduced by measuring the volume of machined lines ore squares followed by least square fits as shown in Fig. 2. However for systematic studies ϕ_{th} and δ can also be deduced by machining single craters with different peak fluences. A least square fit to the measured crater depths in the center according to (1) then leads to these material parameters and finally with (5) to the maximum removal rate.
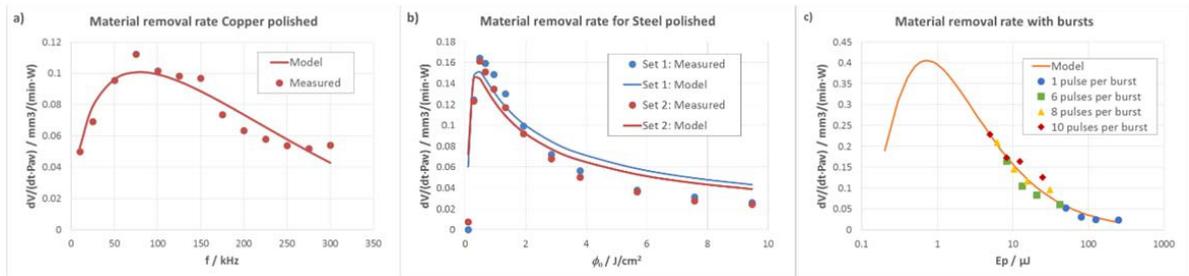

Fig. 2. (a): Removal rate for polished Copper. The removal rate was deduced from the cross section of straight lines machined with constant average power but different repetition rates. The distance between two pulses and the number of repetitions was constant. The dots denote the measured values whereas the solid line represents a least square fit to these data according (3). (b): Results from machining squares into polished stainless steel 1.4301 with different peak fluences. The removal rate was deduced from the depth of the squares machined with constant distance between two pulses, hatch distance and number of repeats. The dots denote the measured values whereas the solid line represents the corresponding least square fits to these data according (4) (c): Material removal rate for steel machined with 50W average power and pulse bursts deduced from the data published in [20] (dots) and the least square fit (solid line) with an adapted model deduced from (4).

2.2. Dependence on the number of pulses; incubation

Already for ns-pulses it was found that the threshold fluence depends on the number of pulses which are applied at one position [24]. Here it was found that the threshold fluence ϕ_{th} changes with the number of pulses N following

$$\phi_{th}(N) = \phi_{th}(1) \cdot N^{S-1} \tag{7}$$

With $\phi_{th}(1)$ the single shot ablation threshold and S the incubation coefficient. In [24] the incubation is related to the storage cycle of thermal stress-strain energy i.e. accumulation of plastic deformation induced by the laser pulses. If $S=1$ incubation is absent whereas for values between 0 and 1 the material is softening and for values above 1 it is hardening. For metals the factor S is typically between 0 and 1, meaning the threshold fluence decreases with increasing number of pulses. This model fits the deduced threshold fluences quite well and was also confirmed (with $S<1$) for ultra-short pulses in the fs regime for metals [25,26,27], semiconductors [28] and transparent materials [29,30]. In this regime it is not clear if the explanation with the thermal stress-strain energy [24] is still applicable. Increased absorption arising from a rougher surface due to formed ripples [31] is an alternative approach to explain the nature of the incubation. In all these publications the energy penetration depth δ is not included in the analysis but this parameter is of great importance as described in the previous section. In [21,22,32] it has been shown that the energy penetration depth is subject to incubation as well and that its behavior follows the threshold fluence as illustrated in fig. 3. The dotted line indicates the fit with the standard model (power function) according to (7). As it can be seen this model especially does not fit the measured values at low pulse numbers, therefore it was supplemented with a constant offset i.e. the threshold value and the penetration depth at infinite number of pulses:

$$\phi_{th}(N) = \phi_{th,\infty} + \Delta\phi_{th} \cdot N^{n_\phi} \text{ and } \delta(N) = \delta_\infty + \Delta\delta \cdot N^{n_\delta} \tag{8}$$
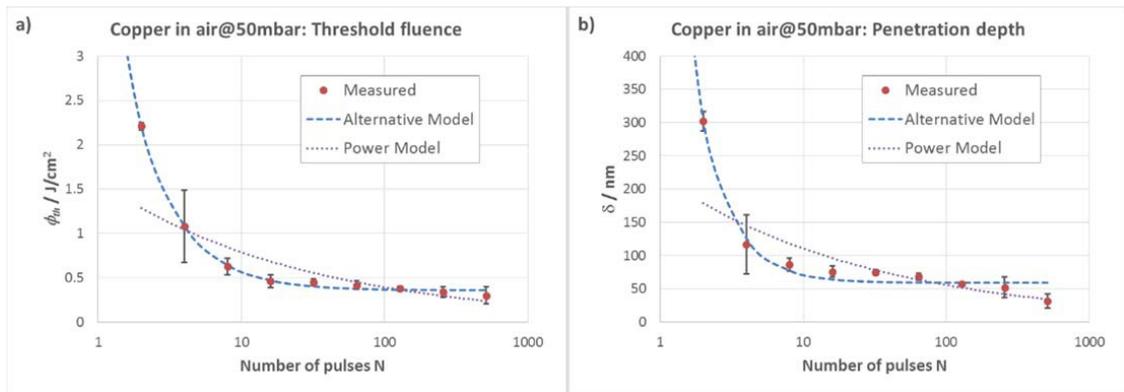

Fig. 3. Threshold fluence (a) and energy penetration depth as a function of the number of pulses applied for polished copper in air at a pressure of 50mbar. The dots denote the measured values with 3σ error bars deduced from a jack-knife analysis. The dotted lines represent the linear regression with a power function according to (7). The incubation coefficient S amounts 0.7 for the threshold fluence and for the penetration depth as well. The dashed line represents the least square fit to the alternative model (8).

Similar behavior is obtained for all investigated metals, gases and pressures in [32]. Assuming that the lateral energy transfer can be neglected and that the evaporation starts after the deposition of the energy the threshold fluence can be expressed by the surface reflectivity R, the energy penetration depth δ, the density ρ and the specific heat of evaporation Ω_{vap} [32]:

$$\phi_{th} = \frac{\delta}{1-R} \cdot \rho \cdot \Omega_{vap} \tag{9}$$

A single variation of the absorption or reflection without influence onto the material should therefore only affect the threshold fluence whereas material changes like surface oxidation, plastic deformations etc. should affect the energy penetration depth and directly scale the threshold too following (9). Comparing $\phi_{th}(N)$ with $\delta(N)$ would in principal allow to distinguish between these two mechanism. In [32] a tendency to a lower reflectivity at high pulse numbers was observed, however additional experiments have to be performed to back up this assumption. Finally the change of the energy penetration depth seems to be the main reason for the change in the threshold fluence and therefore, following (5), the maximum removal rate is less affected by the incubation.

2.3. Influence of the pulse duration

Beside the number of pulses the threshold fluence and the energy penetration depth are affected by the pulse duration as well. Following [13,14,33] one expects a constant threshold fluence for pulse durations shorter than a few ps followed by an increase which is proportional to the square root of the pulse duration for longer pulses. In [11] the ablation of copper for pulse durations between 150fs and 14.4ps at a wavelength of 780nm was investigated and ϕ_{th} and δ were deduced. It was found, that for pulses shorter than 1ps two ablation regimes exist. The first at low fluences, where the energy transport is described by the optical penetration depth. In this regime the threshold fluence is low and the energy penetration depth corresponds to the optical penetration depth $1/\alpha$. In the second regime at higher fluence the energy transport is described by the electron heat penetration depth, which depends on the pulse duration. The reported threshold fluences for a 150fs pulse were $0.14J/cm^2$ in the first regime and $0.46J/cm^2$ in the second regime, respectively. Following (6) the optimum fluence for the first regime already lies in the second one i.e. working at maximum efficiency is only possible for the second regime. Taking into account that industrial ready ultra-short pulsed laser systems have pulse durations of several 100fs and more, the used fluences for laser micromachining are almost exclusively located in the second regime. It is additionally shown that for pulses from 5ps – 15ps the energy penetration depth decreases with increasing pulse duration, a fact which is also confirmed by [21,22] for pulses from 10ps up to 100ps. Systematic studies for shorter pulses are presented e.g. in [34,35,36]. The results of [21,22,34,35] for copper and steel are summarized in fig. 4 and fig. 5, respectively. As expected the threshold fluence is almost constant for pulse durations shorter than 10ps and begins to increase for longer pulses. This increase is more pronounced for steel where the electron-phonon coupling time is 5-10 times lower compared to copper. For both metals (and also for brass investigated in [34]) the energy penetration depth generally increases with decreasing pulse duration as can be seen from fig. 4b and fig. 5b. Following (5) the maximum removal rate should therefore increase with shorter pulse duration. Ths increase is still present for pulses shorter than 10ps where the threshold rests almost constant. Similar dependence of the removal rate from the pulse duration has also been observed for silicon, germanium, zirconium oxide (ZrO_2), polyether ether ketone (PEEK) and polycystalline diamond (PCD). For all these materials an increase of the removal rate with decreasing pulse duration was observed. But also different behavior is possible as e.g. shown for soda lime glass in [35] where the removal rate drops down for very short pulse durations.
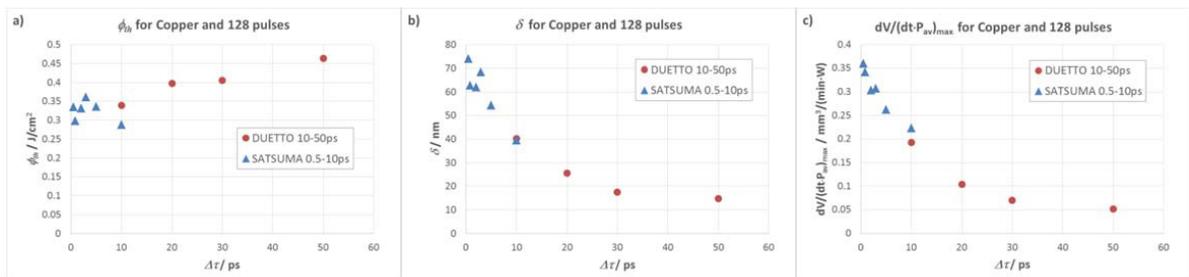

Fig. 4. (a) Threshold fluence (b) energy penetration depth and (c) deduced maximum removal rate (5) for copper and 128 pulses as a function of the pulse duration between 500fs and 50ps. One series of experiments were performed with an adapted DUETTO ps-system and the second series with a SATSUMA fs system; please refer to [34,35] for further experimental details.
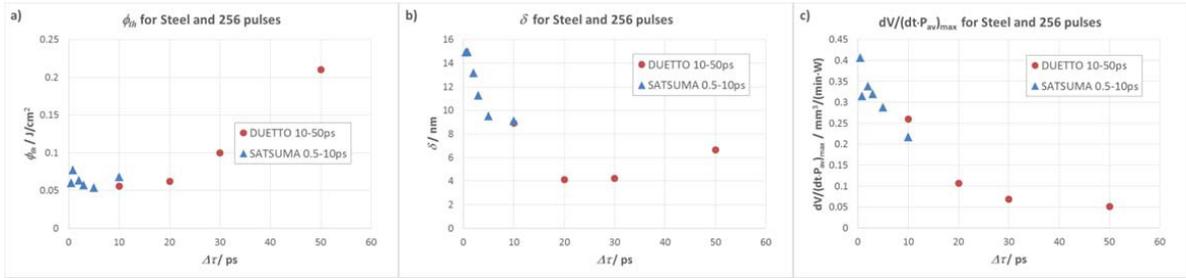
Fig. 5. (a) Threshold fluence (b) energy penetration depth and (c) deduced maximum removal rate (5) for steel 1.4301 and 256 pulses as a function of the pulse duration between 500fs and 50ps. One series of experiments were performed with an adapted DUETTO ps-system and the second series with a SATSUMA fs system; please refer to [34,35] for further experimental details.

In the opposite direction the removal rate rests quite low when the pulse duration is further increased to several 100ps or even to a few ns. Fig. 6 shows the summary of all measured removal rates for different pulse durations. The corresponding experiments were performed at different wavelengths and with different laser systems. The values for the measurements with the Duetto, the Satsuma and the Pharos system were obtained following (5) and measuring ϕ_{th} and δ with the crater method, whereas the values for the series denoted with "divers" are obtained from machining squares (see fig. 2b). The tendency is clearly visible: The removal rate is highest for pulse durations of 2ps and less, significantly drops between 2ps and 50ps, further drops but less pronounced for a few 100ps and slightly increases in the ns-regime. It has to be clearly stated: Despite the low removal rate, pulse durations between a few 10ps and the ns-regime may be of interest due to more cost effective available laser sources or reduced crater cone or CLP formation for steel and semiconductors.
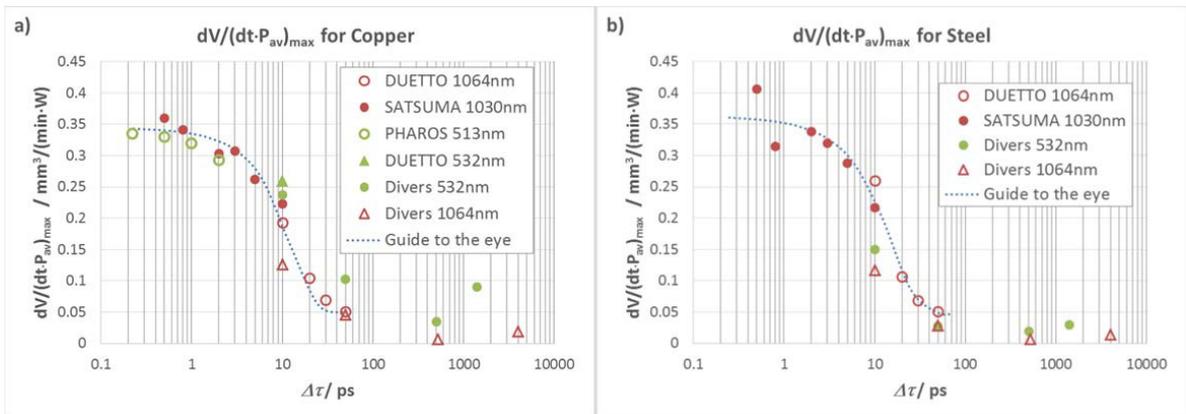

Fig. 6. Maximum removal rate for (a) copper and (b) steel for pulse durations between 250fs and 4ns.

3. Consequences

Following expression (5) the removal rate directly scales with the average power when the fluence is kept at its optimum value corresponding to (6) which is also going with a high machining quality. Keeping the fluence constant means that either the repetition rate or the spot radius has to be increased for a rising the average power. Marking lines serves as the basis for almost all possible surface structuring processes, thus the marking speed v is a very important parameter. A short calculation for the marking speed at the optimum fluence leads to:

$$v = \frac{4}{\pi \cdot e^2} \cdot \frac{(1-o) \cdot P_{av}}{w_0 \cdot \phi_{th}} = 2 \cdot w_0 \cdot (1-o) \cdot f_{opt} \tag{10}$$

With o the spatial overlap between two consecutive pulses. Standard beam guiding systems as e.g. galvo-scanners have marking speeds limited to about 10m/s with a standard $f = 100$mm objective. Thus, when this maximum speed is achieved a further rise of the average power is only possible by an increased spot radius w_0 or spatial overlap o. But the spot radius can't be changed in any order because tight focusing is needed for machining of small structures as the minimum feature size is in the range of one half to one spot radius [37]. One has therefore to increase the overlap o for working with high average power and conventional beam guiding systems. For example machining steel having a threshold fluence of about 0.05J/cm^2 with spot radius of w_0=10μm and an average power of 50W the overlap amounts 99.4% at a marking speed of 10m/s and the repetition rate amounts more the 86MHz (this value corresponds to a typical repetition rate of a seed oscillator). Following [38] this would correspond to a temperature increase of more than 5'000°C due to heat accumulation leading to a surface temperature far above the melting point. In [37] it has further been shown, that minimum surface roughness is achieved with distance from pulse to pulse of half to one spot radius i.e. a spatial overlap of 50-75%. Hence, working with a conventional beam guiding system and a tight spot is limited to a few Watt of average power. The use of today high power systems does not make sense in this case but this could be the market for either more cost effective systems even the efficiency is lower or for a new generation of ps and fs systems having average powers of only a few Watt but with significantly reduced prices compared to today.

4. Actual technologies for high throughput

4.1. General

The previous section has shown the limitations for obtaining high throughput with high power systems and conventional beam guiding systems. There are possibilities to overcome this bottleneck first to work with multi-spot processing and second to use new fast scanning devices and combinations of them.

4.2. Multi-spot processing

The demand to the marking speed can be reduced with multiple of spots. In a first approximation the average power in (10) can be replaced by the average power divided by the number of used spots P_{av}/N. DOEs can be used to generate a pattern with a defined number of mxn spots. This method allows parallel processing of identical structures in the dimension of the spot separation achieved by the DOE. Applications in structuring of solar cells are e.g. described in [39,40,41] and a first multi beam scanner is available via [42]. However, this technology is limited to parallel processing of identical structures.

Variable DOEs as e.g. spatial light modulators (SLM) offer more flexibility for laser micro machining. Here the spot pattern and the spot number can be changed dynamically which allows much more flexible approaches as shown in [43-49]. Also the generation of specific intensity distributions in the focal point as e.g. a triangular top hat is possible [50]. But at the moment the available SLMs are limited in speed with about 50Hz refresh rate and also in maximum pulse energy. However, SLMs are a very promising approach for future applications.

In general multi-spot processing allows the laser to work at lower repetition rates and higher energy as the average power is distributed onto several beams. This also reduces the demands to the gating module (acousto-optic or electro-optic modulator) often placed after the last amplifier stage.

4.3. Fast scanning

Another approach to fulfill the demands for high average power are fast scanning devices. High surface speeds are offered by fast rotating cylinders which can be combined with additional acousto-optic deflectors [51] or be completely synchronized with the laser system [52,53].

More flexible are fast rotating polygon scanners which offer marking speeds up to the speed of sound [54,55]. In this case the beam scans a straight line of a given length with a constant speed. The movement perpendicular to the scan direction is either realized with a galvo mirror in front of the polygon wheel or with a linear axis which moves

the machined sample. With a second galvo mirror in front of the polygon wheel the facet error is corrected. Due to their high marking speed these system really offer the possibility to work with average powers exceeding 100W.

An alternative approach for a polygon scanner set up was presented in [56] and new products will be launched soon [57]. They offer marking speeds up to 100m/s and can additionally be synchronized with the laser system. Experiments were performed with a Fuego 40W ps-laser-system offering repetition rates up to 8.2MHz and a spot diameter of about 50μm. It has been shown that stainless steel 1.4301 can be machined with more than 40W of average power at the maximum repetition rate of the system by generating 3D pyramids into the surface [58,59]. The obtained results are very encouraging and strategies have been developed to deal with the still existing problems like the pyramidal error and the limitation to pick single pulses at high repetition rates in the MHz regime. E.g. in an experiment the topography of Switzerland [60], acting as a real 3D-structure, was machined into stainless steel 1.4301 with 25.6W average power (measured in front of the polygon scanner) at a repetition rate of 4.1MHz. The corresponding scan speed amounted 59.45m/s corresponding to a pulse to pulse distance of 14.5μm i.e. an overlap of about 75%. The structuring was performed at the optimum fluence, a facet-averaging strategy, and 2233 different layers. The final result without any post processing is shown in Fig. 7. The dimensions are 107.7mm x 65.5mm with a maximum depth of about 115μm.

For the used repetition rates of several 100kHz up to 8.2MHz particle shielding, described in [61-63], can appear and may reduce the process efficiency, e.g. a reduction of about 30% for steel was measured in [59,64]. Additionally heat accumulation is expected to lead to a slightly increasing removal rate for repetition rates of a few MHz. Further experiments are in progress to investigate these findings and to identify the influence of material parameters to the particle shielding effect and the heat accumulation. Smaller spots and even higher average powers would allow to investigate other metals like copper or brass at average powers up to 100W in the future. Also shorter pulse durations will be used to test if the expected gain in the removal rate can be realized.
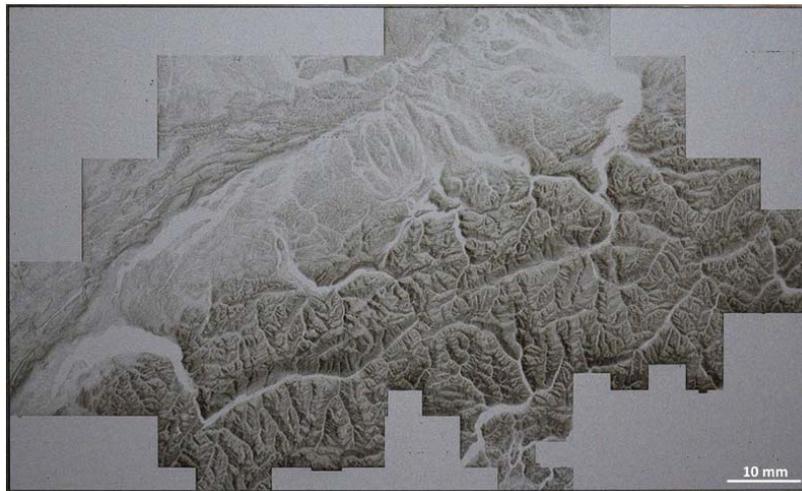

Fig. 7. Photography of the machined topography of Switzerland in stainless steel.

5. Conclusion

For ultra-short pulses the threshold fluence ϕ_{th} and the energy penetration depth δ are the two main factors describing the ablation process. The removal rate can be maximized if the optimum fluence is applied; for a Guassian beam the optimum peak fluence reads $\phi_0 = e^2 \cdot \phi_{th}$. Both, the threshold fluence and the energy penetration depth are subject to the incubation effect i.e. they decrease with the number of pulses applied. Therefore the maximum removal rate is rather little affected by the incubation effect. Significantly higher is the influence of the pulse duration. It leads, for metals, to a higher energy penetration depth for shorter pulses resulting in a higher removal rate in the fs-regime. In contrast the energy penetration depth significantly drops for longer pulses. Together

with the increasing threshold fluence this leads to a strong drop in the removal rate for pulses longer than approximately 10ps.

As the threshold fluence for metals is quite low (several $0.1 J/cm^2$ or even less) the corresponding optimum fluence rests moderate too. As tight spot sizes are used to machine small structures this leads to very high repetition rates at high average powers. To avoid heat accumulation and to obtain low surface roughness demand therefore very high marking speeds as they can be offered on fast rotating cylinders or by polygon scanners. With the latter laser machining of steel with ps pulses up to an average power exceeding 40W at a repetition rate of 8.2MHz was demonstrated. Another approach to work with high average power is to divide the energy into multiple beams with a diffractive optical element. Both methods open the door for using high average powers of 100W and more but additional work has still to be done.

On the other hand more cost effective systems with higher pulse durations even showing significantly lower removal rates could be of interest as they can be used with standard beam guiding systems e.g. galvo-scanners. This could also be very attractive for fs and ps systems with only a few Watt average power if they could be produced for significantly lower prices in near future.

However, today fast scanning systems or multi-spot processing are the most promising technologies for surface structuring with high throughput.

Acknowledgements

References

[1] P. Russbueldt, T. Mans, J. Weitenberg, H.-D. Hoffmann, R. Poprawe, "Compact diode-pumped 1.1 kW Yb:YAG Innoslab femtosecond amplifier," Opt. Lett. 35, 4169-4171 (2010)
[2] P. Russbueldt, T. Mans, H-D. Hoffmann, R. Poprawe, "1100 W Yb:YAG femtosecond Innoslab amplifier", Proc. of SPIE, 7912 (2011)
[3] J.-P. Negel et al., "1.1 kW average output power from a thin-disk multipass amplifier for ultrashort laser pulses", Optics Letters, 38 4, 5442-5445 (2013)
[4] S. Pierrot, J. Saby, B. Cocquelin and F. Salin, "High-Power all Fiber Picosecond Sources from IR to UV", Proc. of SPIE Vol. 7914 (2011)
[5] S. Kanzelmeyer, H. Sayinc, T. Theeg, M. Frede, J. Neumann and D. Kracht, "All-fiber based amplification of 40 ps pulses from a gain-switched laser diode", Proc. of SPIE Vol. 7914 (2011)
[6] P Deladurantaye, A. Cournoyer, M. Drolet, L. Desbiens, D. Lemieux, M. Briand and Y. Taillon, "Material micomachining using bursts of high repetition rate picoseconds pulses from a fiber laser source", Proc. of SPIE Vol. 7914 (2011)
[7] M. Ryser, M. Neff, S. Pilz, A. Burn, V. Romano, "Gain-switched laser diode seeded Yb-doped fiber amplifier delivering 11-ps pulses at repetition rates up to 40-MHz", Proc. of SPIE Vol. 8237 (2012)
[8] B.N. Chichov, C. Momma, S. Nolte, F. van Alvensleben and A. Tünnermann, "Femtosecond, picosecond and nanosecond laser ablation of solids", Applied Physics A, 63, 109-115 (1996)
[9] C. Momma, B.N. Chichkov, S. Nolte, F. v. Alvensleben, A. Tünnermann, H. Welling, B. Wellegehausen, „Short-Pulse Laser Ablation of Solid targets", Opt. Comm., 129, 134 – 142 (1996)
[10] C. Momma, S. Nolte, B. N. Chichkov, F. v. Alvensleben, A. Tünnermann, "Precise laser ablation with ultrashort pulses", Appl. Surf. Sci., 109/110, 15 – 19 (1997)
[11] S. Nolte, C. Momma, H. Jacobs, A. Tünnermann, B.N. Chichkov, B. Wellegehausen, H, Welling, „Ablation of metals by ultashort laser pulses", J. Opt. Soc. Am. B, 14, 2716 – 2722 (1997)
[12] A. P. Kanavin, I. V. Smetanin, V. A. Isakov, Yu. V. Afanasiev, B. N. Chichkov, B. Wellegehausen, S. Nolte, C. Momma, A. Tünnermann, „Heat transport in metals irradiated by ultrashort laser pulses", Phys. Rev. B, 57, 14 198 – 14 703 (1998)
[13] G. Mourou et al., "Method for controlling Configuration of laser induced breakdown and ablation", US Patent US RE37,585 E, (2002)
[14] F. Dausinger, H. Hügel, V. Konov, "Micro-machining with ultrashort laser pulses: From basic understanding to technical applications", Proc. of SPIE 5147, 106-115 (2003)
[15] D. Breitling, A. Ruf, F. Dausinger, "Fundamental aspects in machining of metals with short and ulrashort laser pulses", Proc. of SPIE 5339, 49-63 (2004)
[16] G. Raciukaitis, M. Brikas, P. Gecys, B. Voisiat, M Gedvilas, „Use of high repetition rate and high power lasers in microfabrication: How to keep the efficiency high?", JLMN journal of Laser Micro/Nanoengineering Vol. 4, 186 (2009)
[17] B. Neuenschwander, G. Bucher, Ch. Nussbaum, B. Joss, M. Muralt, U. Hunziker, P. Schuetz, „Processing of metals and dielectric materials with ps-laserpulses: results, strategies, limitations and needs", Proc. of SPIE 7584-26 (2010)
[18] B. Neuenschwander, B. Jaeggi, M. Schmid, „From fs to sub-ns: Dependence of the Material Removal Rate on the Pulse Duration for Metals", Physics Procedia Vol. 41, pp. 787-794 (2013)
[19] B. Neuenschwander, G. Bucher, G. Hennig, Ch. Nussbaum, B. Joss, M. Muralt, S. Zehnder, U. Hunziker, P. Schuetz, „Processing of dielectric materials and metals with ps-laserpulses", Proc. of ICALEO, M101 (2010)

[20] R. Knappe, H. Haloui, A. Seifert, A. Weis, A. Nebel, „Scaling ablation rates for picosecond lasers using burst micromachining", Proc. of SPIE 7585-16 (2010)

[21] M. Schmid, B. Neuenschwander, V. Romano, B. Jaeggi, U. Hunziker, „Processing of metals with ps-laser pulses in the range between 10ps and 100ps", Proc. of SPIE 7920-08 (2011)

[22] B. Jaeggi, B. Neuenschwander, M. Schmid, M. Muralt, J. Zuercher, U. Hunziker, "Influence of the pulse duration in the ps-regime on the ablation efficiency of metals", Physics Procedia Vol. 12B, pp. 164-171 (2011)

[23] B. Lauer, B. Neuenschwander, B. Jaeggi, M. Schmid, „ From fs – ns: influence of the pulse duration onto the material removal rate and machining quality for metals", Proc. of ICALEO M309 (2013)

[24] Y. Jee, M.F. Becker and R.M. Walser, "Laser-induced damage on single-crystal metal surfaces", J. Opt. Soc. Am. B, 5 (1988)

[25] P.T. Mannion, J. Magee, E. Coyne, G.M. O'Connor, T.J. Glynn, "The effect of damage accumulation behavior on ablation thresholds and damage morphology in ultrafast laser micro-machining of common metals in air," Appl. Surf. Sci. 233, pp 275 – 287 (2004)

[26] S.E. Kirkwood, A.C. Van Popta, Y.Y. Tsui, R. Fedosejevs, "Single and multiple shot near-infrared femtosecond laser pulse ablation thresholds of copper," Appl, Phys. A, 81, pp 729 – 735 (2005)

[27] J. Byskov-Nielsen, J.M. Savolainen, M.S. Christensen, P. Balling, „Ultra-short pulse laser ablation of metals: threshold fluence, incubation coefficient and ablation rates," Appl. Phys. A, 101, pp 97 – 101 (2010)

[28] J. Bonse, J.M. Wrobel, J. Krüger W. Kautek, "Ultrashort-pulse laser ablation of indium phosphide in air," Appl. Phys. A; Vol. 72, pp 89 – 94 (2001)

[29] A. Rosenfeld, M. Lorenz, R. Stoian D. Ashkenasi, "Ulrashort-laser-pulse damage threshold of transparent materials and the role of incubation," Appl. Phys. A; Vol. 69 [Suppl.], 373 – 376 (1999)

[30] M- Lenzer, J. Krueger, W. Kautek F. Krausz, „Incubation of laser ablation in fused silica with 5-fs pulses," Appl. Phys. A, 69, pp 456 – 466, (1999)

[31] R. Lausten, J.A. Olesen, K. Vestentoft, P. Balling, „Ultrafast Phenomena XIII" Springer Series in Chemical Physics 71, p 675 (2002)

[32] B. Neuenschwander, B. Jaeggi, M. Schmid, A. Dommann, A. Neels, T. Bandi, G. Hennig, "factors controlling the incubation in the application o fps laser pulses on copper and iron surfaces", Proc. of SPIE 8607-12 (2013)

[33] G. Mourou et al., "Method for controlling Configuration of laser induced breakdown and ablation", US Patent US RE37,585 E (2002)

[34] B. Neuenschwander, B. Jaeggi, M. Schmid, V. Rouffiange, P. E. Martin, „Optimization of the volume ablation rate for metals at different laser pulse-durations from ps to fs",Proc. of SPIE 8243-6 (2012)

[35] B. Neuenschwander, B. Jaeggi, M. Schmid, „From ps to fs: Dependence of the material removal rate and the surface quality on the pulse duration for metals, semiconductors and oxides", Proc. of ICALEO M1004 (2012)

[36] J. Lopez, A. Lidolff, M. Delaigue, C. Hönninger, S. Ricaud and E. Mottay, "Ultrafast Laser with highEnergy and high average power for Industrial Micromachining: Comparision ps-fs", Proc. of ICALEO M401 (2011)

[37] B. Jaeggi, B. Neuenschwander, U. Hunziker, J. Zuercher, T. Meier, M. Zimmermann, K.H. Selbmann, G. Hennig, „Ultra high precision surface structuring by synchronizing a galvo scanner with an ultra short pulsed laser system in MOPA arrangement", Proc. of SPIE, 8243-20 (2012)

[38] R. Weber, Th. Graf, P. Berger, V. Onuseit, M. Wiedenmann, Ch. Freitag, A. Feurer, „Heat accumulation during pulsed laser materials processing", accepted for publication in Optics Express (2014)

[39] A. Schoonderbeek V. Schuetz, O. Haupt, U. Stute, „Laser Processing of Thin Films for Photovoltaic Applications", JlMN Vol. 5, pp. 248 – 255 (2010)

[40] O. Haupt, V. Schuetz, U. Stute, "Multi-Spot Laser Processing of Crystalline Solar Cells", Proc. of SPIE 7921 (2011)

[41] V. Schuetz, A. Horn, U. Stute, „High-throughput process parallelization for laser surface modification on Si-Solar cells: determination of the process window", Proc. of SPIE 8244 (2012)

[42] Pulsar Photonics, http://www.pulsar-photonics.de/?page_id=719

[43] S. Torres-Peiro,J. Gonzalez-Ausejo, O. Mendza-Yero, "Parallel laser micromachining based on diffractive optical elements with dispersion compensated femtosecond pulses", Opt. Exp. 21, pp. 31830-31836 (2013)

[44] Z. Kuang, W. Perrie, J. Leach, M. Sharp, S.P. Edwardson, "High throughput diffractive multi-beam femtosecond laser processing using a spatial light modulator", Appl. Surf. Sci. 255, pp.2284-2289 (2008)

[45] Z. Kuang, W. Perrie, D. Liu, S. Edwardson, "Diffractive multi-beam surface micro-processing using 10 ps laser pulses", Appl. Surf. Sci. 255, pp. 9040-9044 (2009)

[46] Z. Kuang, D. Liu, W. Perrie, S. Edwardson, "Fast parallel diffractive multi-beam femtosecond laser surface micro-structuring", Appl. Surf. Sci. Vol. 255, pp. 6582-6588 (2009).

[47] M. Silvennoinen, J. Kaakkunen, K. Paivasaari, "Parallel microstructuring using femtosecond laser and spatial light modulator", Physics Procedia Vol. 41, pp. 693-69 (2013)7

[48] , K. Paivasaari, „Parallel Femtosecond Laser Processing Using Intensity Modulated Diffraction Pattern Produced with Spatial Light Modulator", Proc. of ICALEO M202 (2013)

[49] K. Paivasaari, M. Silvennoinen, J. Kaakkunen, P. Vahimaa, „Femtosecond laser processing and spatial light modulator", Proc. of SPIE 8967 (2014)

[50] R.J. Beck, J.P. Parry, W.N. MacPherson, A. Waddie, N.J. Weston, J.D. Shephard, D.P. Hand, "Application of cooled spatial light modulator for high power nanosecond laser micromachining", Opt. Exp. 18, pp. 17059-17065 (2010)

[51] S. Bruening, G. Hennig, S. Eifel, A. Gillner, „Ultrafast Scan Techniques for 3D-Structuring of Metal Surfaces with high repetitive ps-laser pulses", Physics Procedia Vol. 12 Part B, pp. 105-115 (2011)

[52] B. Jaeggi, B. Neuenschwander, T. Meier, M. Zimmermann, G. Hennig, „High throughput laser micro machining on a rotating cylinder with ultra short pulses at highest precision", Proc. of SPIE 8607 (2013)

[53] B. Jaeggi, B. Neuenschwander, T. Meier, M. Zimmermann, G. Hennig, „High Precision Surface Structuring with Ultra-Short Pulses and Synchronized Mechanical Axes", Physics Procedia Vol. 41, pp. 319-326 (2013)

[54] Fraunhofer ILT: http://www.ilt.fraunhofer.de/content/dam/ilt/de/documents/Jahresberichte/JB11/JB11_S51.pdf

[55] Fraunhofer ILT: http://www.ilt.fraunhofer.de/de/publikationen-und-presse/jahresberichte/2012/jahresbericht-2012-s110.html

[56] R. De Loor, "Polygon scanner system for ultra short pulsed laser micro-machining applications", Physics Procedia Vol. 41, pp. 544-551 (2013)

[57] NextScan Technology: http://nextscantechnology.com/2014-product-release/

[58] B. Neuenschwander, B. Jaeggi, M. Zimmermann, L. Penning, R. De Loor, K. Weingarten, A. Oehler, "High throughput surface structuring with ultrashort pulses in synchronized mode with fast polygon line scanner", Proc. of ICALEO M203 (2013)

[59] B. Neuenschwander, B. Jaeggi, M. Zimmermann, L. Penning, R. De Loor, K. Weingarten, A. Oehler, „High-throughput and high-precision laser micromachining with ps-pulses in synchronized mode with a fast polygon line scanner", Proc. of SPIE 8967 (2013)

[60] Bundesamt fuer Landestopografie: http://www.swisstopo.ch/

[61] J. Koenig, S. Nolte, A. Tuennermann, "Plasma evolution during metal ablation with ultrashort laser pulses", Opt. Exp. 13, pp 10597-10607 (2005)

[62] S. Nolte, C. Schaffer, "Micromachining with Femtosecond Lasers", SPIE Education Services (2012)

[63] A. Ancona, F. Roeser, K. Rademaker, J. Limpert, S. Nolte, A. Tuennermann, "High speed laser drilling of metals using a high repetition rate, high average power ultrafast fiber CPA system" Opt. Exp. 16, 8958-8968 (2008)

[64] B. Jaeggi, B. Neuenschwander, M. Zimmermann, R. De Loor, L. Penning, „High throughput ps-laser micro machining with a synchronized polygon line scanner", to be published in Physics Proceedia